

See discussions, stats, and author profiles for this publication at: <https://www.researchgate.net/publication/372451951>

Using novel click chemistry algorithm to design D₃R inhibitors as blood-brain barrier permeants

Article in Future Medicinal Chemistry · July 2023

DOI: 10.4155/fmc-2022-0310

CITATION

1

READS

48

4 authors, including:



[Yuri Porozov](#)

HSE University

75 PUBLICATIONS 1,314 CITATIONS

[SEE PROFILE](#)



[Ekaterina Skorb](#)

Max Planck Institute of Colloids and Interfaces

180 PUBLICATIONS 3,536 CITATIONS

[SEE PROFILE](#)



[Sergey Shityakov](#)

University of Wuerzburg

165 PUBLICATIONS 1,841 CITATIONS

[SEE PROFILE](#)

Using novel click chemistry algorithm to design D3R inhibitors as blood–brain barrier permeants

Alexander A Kovalenko¹, Yuri B Porozov^{2,3} , Ekaterina V Skorb¹ & Sergey Shityakov^{*,1} 

¹Infochemistry Scientific Center, ITMO University, Lomonosova Street 9, Saint Petersburg, 191002, Russian Federation

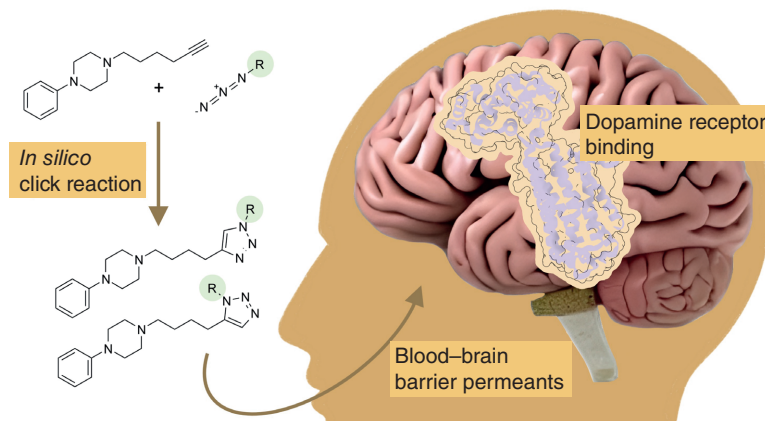
²Center of Bioinformatics and Chemoinformatics, IM Sechenov First Moscow State Medical University, Bol'shaya Pirogovskaya Street 2, Moscow, 119991, Russian Federation

³HSE University, Kantemirovskaya Street 3A, Saint Petersburg, 194100, Russian Federation

*Author for correspondence: shityakoff@hotmail.com

Dopamine receptor D3 (D3R) has gained attention as a promising therapeutic target for neurological disorders. In this study, an innovative *in silico* click reaction strategy was employed to identify potential D3R binders. The ligand template, 1-phenyl-4-[4-(1H-1,2,3-triazol-5-yl)butyl]piperazine, with substitution at the 1,2,3-triazole ring, served as the starting point. Generated compounds underwent filtration based on their brain-to-blood concentration ratio (logBB), leading to the identification of 1-[4-[1-(decahydronaphthalen-1-yl)-1H-1,2,3-triazol-5-yl]butyl]-4-phenylpiperazine as the most promising candidate, displaying superior D3R affinity and blood–brain barrier (BBB) permeability compared to the reference ligand, eticlopride. Molecular dynamics simulations further supported these findings. This study presents a novel hit for designing D3R ligands and establishes a workflow utilizing *in silico* click chemistry to screen compounds with BBB permeability. The proposed click reaction-based algorithm holds significant potential as a valuable tool in the development of effective antipsychotic compounds.

Graphical abstract:



First draft submitted: 30 December 2022; Accepted for publication: 22 May 2023; Published online: 19 July 2023

Keywords: blood–brain barrier • click chemistry • Dopamine receptor D3 • D3R • virtual screening

There has been growing interest in recent decades in dopamine receptors as targets for the treatment of neurological and psychiatric disorders [1]. This group of G-protein-coupled receptors is generally responsible for mediation of

**newlands
press**

dopamine activity in the central nervous system (CNS) and is expressed over numerous areas of the brain and its periphery [2]. Two main dopamine receptor groups differing in localization, binding patterns and physiological roles are distinguished: D1-like receptors (D1R and D5R) and D2-like receptors (D2R, D3R and D4R). D3R, in particular, is located in the limbic areas: the shell of the nucleus accumbens, the olfactory tubercle, the islands of Calleja and (with lower density) the dorsal striatum's medium spiny neurons [3,4]. D3R functions build at both presynaptic and postsynaptic levels and are complex in comparison with D1-like receptors [2]. D3R participates in locomotor activity regulation, influences some specific aspects of cognitive functions that are mediated by hippocampal areas and is also critically involved in reward and reinforcement mechanisms and emotional and endocrine functions [4,5]. Evidence suggests that D3 receptor-dependent neurotransmission plays a crucial role both in preventing the development of pathological alterations and during the progression of neurodegenerative disorders [6,7]. Furthermore, D3R involvement is documented in a number of pathological neurological and psychiatric conditions, including schizophrenia [8], Parkinson's disease [9], addiction [5,10] and anxiety and depression [11]. Beyond the CNS, D3R seems to be involved in the pathological conditions of the eye (ocular hypotension and glaucoma), pancreas (diabetes associated with Parkinson's disease and schizophrenia) and cardiovascular system (hypertensive states, atherosclerosis) [12]. As a result, molecules targeting D3R have potential in the treatment of the aforementioned conditions and have been the subject of numerous studies [1,13].

One of the main obstacles in the discovery of D3R ligands is the high structural similarity of dopamine receptors, with 78% sequence identity, including binding sites [1]. Numerous molecular scaffolds have been explored in the field of rational drug design and discovery. Figure 1A shows a panel of D3R ligands representing such molecular scaffolds. An effective approach to tackling the D2/D3R selectivity issue was found by employing molecules analyzed as pharmacophores [1]. This pharmacophore model provides the ability to investigate a binding pocket, which is composed of residues at helices II–III and VII and has a different conformation from that of D2R (Figure 1B).

A commonly utilized scaffold for ligand design is a substituted 4-phenylpiperazine with a pharmacophore (frequently an aryl ring system) and butylamide linker (Figure 1A) [10,14]. Structure–activity relationship studies proved the importance of a carboxamide moiety [15] and demonstrated that a tetramethylene linker has the optimal length and flexibility to facilitate D3R selective binding [16]. To enhance drug stability, a replacement of the amide moiety with 1,2,3-triazole was proposed, as the amide is thought to be a potential site of metabolism (Figure 1C) [17]. Compounds with this substitution were proven to be prominent templates for the synthesis of selective D3R ligands with increased stability. In addition, the 1,2,3-triazole moiety is easily accessible via copper-catalyzed azide–alkyne cycloaddition synthesis.

Virtual screening of D3R inhibitors has been approached in many ways, including structure-based screening via molecular docking [18], 3D pharmacophore-guided screening [19] and machine learning-aided binder prediction [20]. In this study, the screening of novel D3R binders was explored via *in silico* click chemistry synthesis of compounds with a 1,2,3-triazole moiety. The overview of the screening process is provided in Figure 1C. In consideration of the localizations of D3R in specific brain regions, the screening process was enhanced by incorporating the selection of compounds that are capable of permeating the blood–brain barrier (BBB). This was achieved by filtering molecules based on their estimated logarithmic ratio between brain and blood concentration ($\log\text{BB}$) [21,22].

The 1-phenyl-4-[4-(1H-1,2,3-triazol-5-yl)butyl]piperazine scaffold was employed as a template for identification of ligands with improved bioactivity (Figure 1C). Starting with the template alkyne and a collection of azides obtained from the PubChem database, a library of 1,2,3-triazole compounds was generated and screened for potential D3R binders by D3R docking with AutoDock Vina and iDock. Based on the predictions of two software programs, a panel of potential hits was shortlisted. The hit bearing a decahydronaphthalen-1-yl substituent was identified to have higher binding affinity and BBB permeability than eticlopride, a D2/D3R antagonist commonly used in pharmacological research. Free binding energy estimation using the linear interaction energy (ΔG_{lie}) method, based on molecular dynamics (MD) simulation of the D3R membrane-embedded complex, proved the improved affinity of the hit molecule over the reference ligand. As a result, the workflow for *in silico* screening of D3R ligands as BBB permeants aided by *in silico* click reaction was described and validated. This protocol can be further applied to screen other protein ligands that can be synthesized using the novel combinatorial click chemistry algorithm.

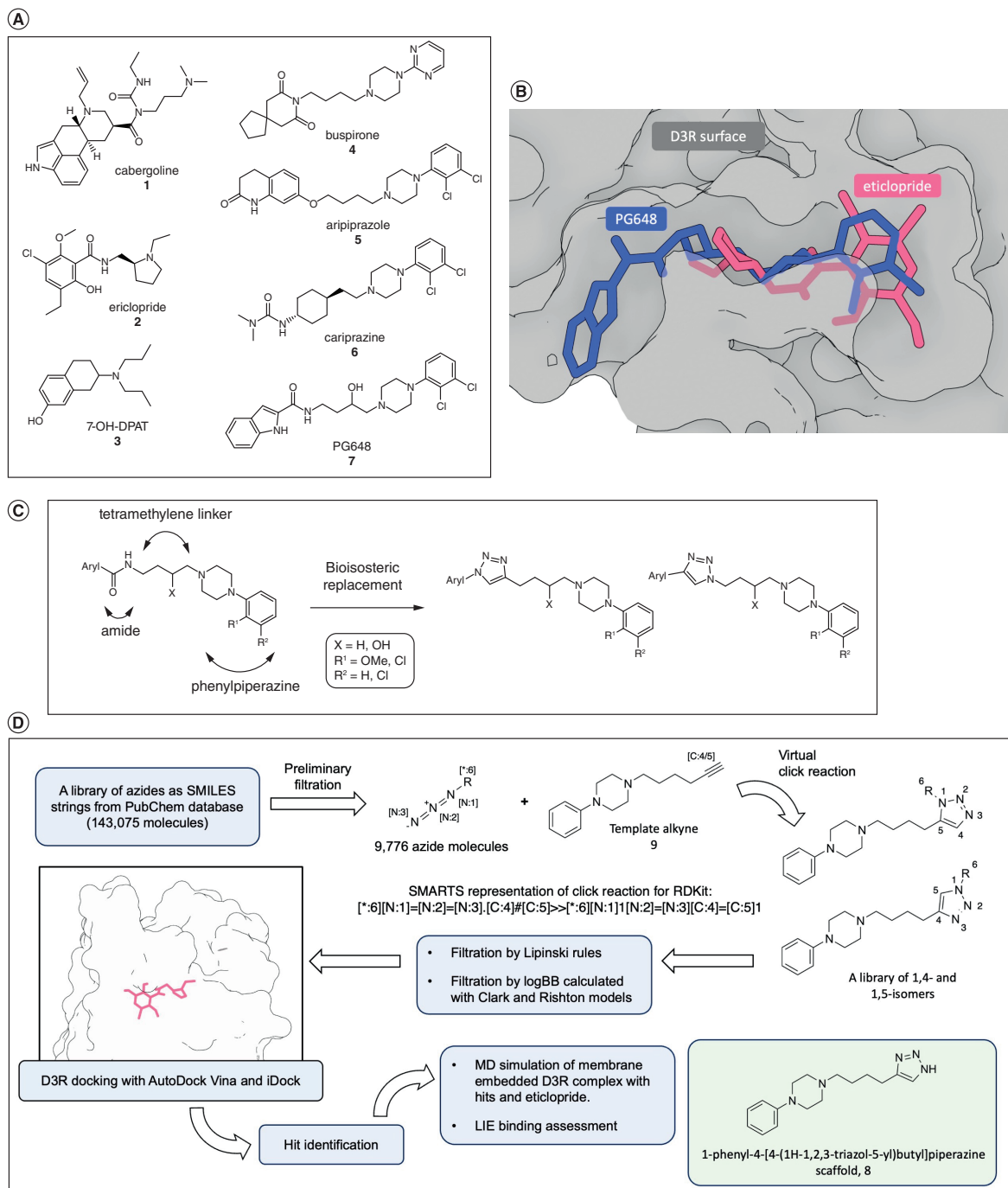


Figure 1. Overview of analyzed ligands and computational methodology. (A) Panel of various D3R ligands. Compound 7 is a proposed ligand. (B) Visualization of eticlopride (magenta) and PG648 (blue) binding modes with D3R predicted by AutoDock Vina. D3R surface is in gray, visualized with the Protein Imager. (C) Bioisosteric replacement of amide moiety by 1,2,3-triazole ring. (D) Workflow for virtual screening of D3R ligands based on the 1-phenyl-4-[4-(1H-1,2,3-triazol-5-yl)butyl]piperazine scaffold. A SMARTS pattern for virtual click reaction producing both 1,4- and 1,5-isomers is shown. Atoms in reagents and products are numbered to illustrate bond formation in RDKit guided by a specified pattern. Data taken from [14,36,17]. LIE: Linear interaction energy; MD: Molecular dynamics.

Results & discussion

A comprehensive PubChem search was conducted to compile an initial library of 143,075 azide molecules, represented as SMILES strings. Subsequently, an initial filtration process was implemented, resulting in a reduction of the library size to 9,776 unique azide molecules. These selected molecules were then subjected to virtual click reaction analysis. Both 1,4- and 1,5-isomers were generated in order to investigate whether there was a binding preference for a particular isomer. Click reaction product generation in RDKit failed for six azide molecules. These compounds appeared to be copies of hydrazoic acid, sulfuryl azide and bis(2-azidoethyl)amine that were unfiltered at the first step. The products of 708 azides did not pass Lipinski's rule filter, and the generator yielded a collection of 18,838 1,2,3-triazole compounds composed of 9419 1,4-isomers and 9419 1,5-isomers. Charts for the distribution of logBB values computed by Clark [23] and Rishton *et al.* [24] equations and Tanimoto similarities in the generated library are provided in Supplementary Figure 1.

The distribution of rotatable bonds across molecules in the library demonstrated that 73% of generated compounds had five to ten rotatable bonds (Figure 2A). This observation is similar to the analysis of 193 drug molecules conducted by Günther *et al.*, which demonstrated that molecules with these amounts of rotatable bonds account for approximately 20% of studied compounds [25]. In this sense, the generated library can be considered relevant for drug molecule search.

Molecules with a logBB value of 0.3 or higher were filtered out during the development of a model to predict BBB permeability, as these molecules are readily permeable through the BBB. This threshold was proposed by Shityakov *et al.* [22] and Kunwittaya *et al.* [26], who studied a large dataset of compounds with known logBB values. Upon applying the filtration step, a total of 230 molecules successfully passed the filtration criteria based on the logBB Clark method. Additionally, using the logBB Rishton method, 3062 molecules were identified as meeting the filtration requirements.

The estimated logBB values for eticlopride were found to be -0.35 (Clark) and -0.02 (Rishton), which are considerably lower than the logBB threshold utilized for library filtration. As a result, molecules that have been shortlisted based on either the Clark or Rishton logBB values are expected to exhibit reasonable permeability across the BBB. It is worth noting that the Rishton equation consistently yields higher logBB estimates compared to Clark's model (Figure 2B). This raises the question of whether it is more advantageous to filter a smaller number of molecules using Clark's model or a larger number using Rishton's model. It is important to highlight that all compounds that passed the filtration based on Clark's logBB values were also included in those filtered by Rishton's model. Subsequently, this subset of 3062 molecules was subjected to screening using molecular docking techniques.

For the D3R docking screening, molecular docking was performed to identify the best ligand binding poses for further analysis. The Vina molecular docking method is a widely used and popular algorithm for predicting the binding modes and affinities of small molecules to protein targets. The Vina algorithm was unable to dock 46 molecules due to the presence of some atoms that were not parameterized in the software. While iDock, which has broader parametrization, successfully docked these molecules, they were excluded from further analysis as they were deemed clinically irrelevant. As a result, the docking data for 3016 molecules were subjected to analysis. Comparing the docking affinities of these molecules with those of the scaffold and eticlopride (Table 1), it was observed that the majority of the studied compounds exhibited higher affinity than the reference molecules (Figure 3A).

iDock leverages the Vina scoring function and optimization algorithm, resulting in a strong correlation of affinities between these two software programs (Figure 3B). Because of the similarity between Vina and iDock scores, the majority of plots are provided for Vina only. The charts for iDock affinities demonstrated similar patterns and are provided in Supplementary Figure 2.

Figure 4C illustrates the distribution of Vina docking scores, highlighting the scores for compounds with Clark's logBB above the 0.3 threshold. The scores of Clark compounds are uniformly distributed across the scores of Rishton compounds. This observation suggests that filtering molecules by Rishton's logBB is more beneficial, as it provides a larger set of BBB-permeable compounds for screening and is also unlikely to produce a lower proportion of affine binders in a subset.

As shown in Figure 3D & E, violin plots were used to compare the distributions of Vina and iDock affinities for 1,4- and 1,5-isomers in the library. These distributions exhibited similarity, with closely aligned quartile values. Paired Student's t-test comparing the means of Vina scores did not show a significant difference ($p\text{-value} = 0.22$). However, in the case of iDock, the test revealed distinct distributions ($p\text{-value} = 5 \cdot 10^{-5}$). Furthermore, the scatter plot depicting Vina affinities for 1,5-isomers against those of the corresponding 1,4-isomers displayed a noticeable

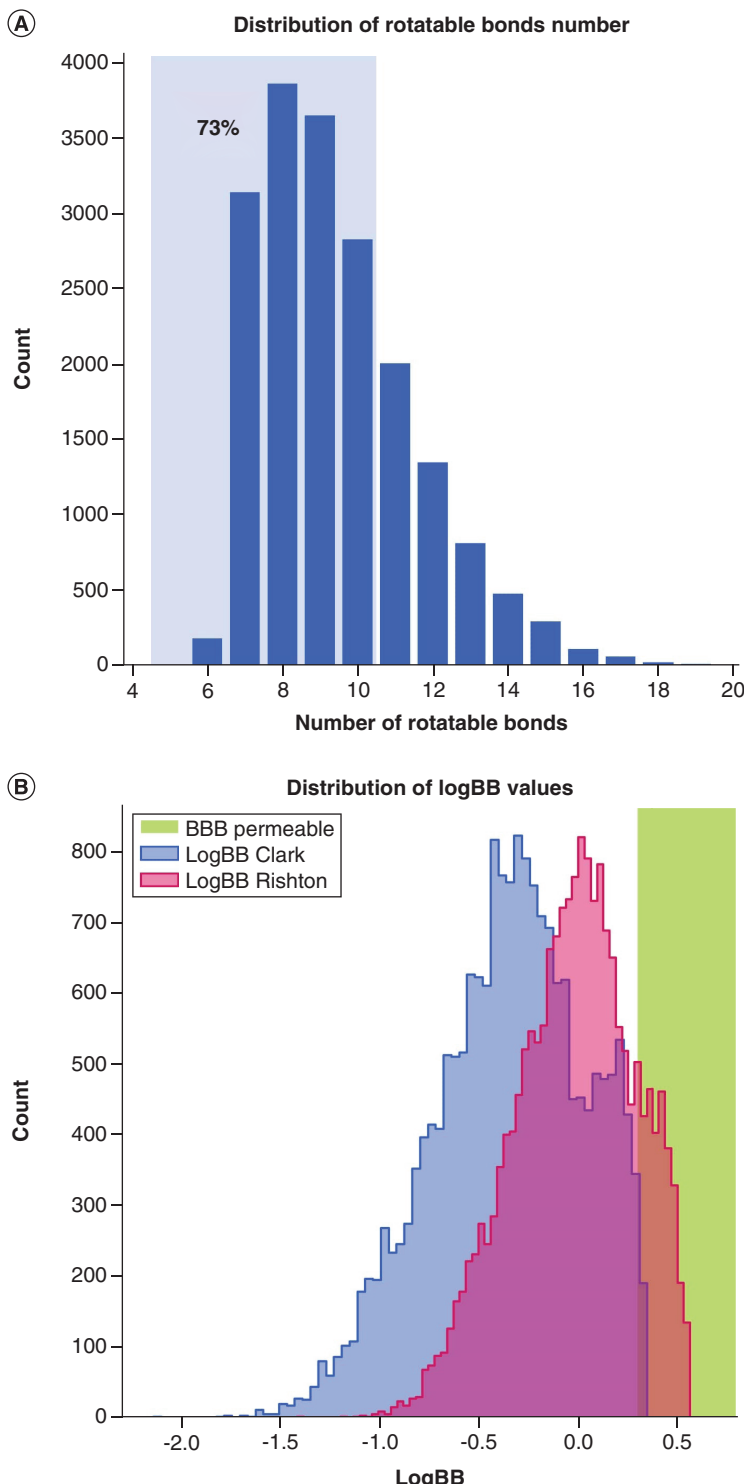


Figure 2. Distribution of parameters in the generated library of 1,2,3-triazole compounds. (A)

Distribution of the number of rotatable bonds across molecules in the library with the proportion of molecules having five to ten rotatable bonds. **(B)** Distribution of logBB values calculated with Clark (blue) and Rishton (red) equations, indicating the difference between these models. The logBB threshold of 0.3 for compounds readily permeable through the BBB is highlighted in green.

BBB: Blood-brain barrier; logBB: Logarithmic ratio between the concentration of a compound in the brain and blood.

Table 1. Vina and iDock binding affinities established for the reference compounds.

Compound	Vina affinity, kcal/mol	iDock affinity, kcal/mol
Scaffold	-7.74 ± 0.04	-7.74 ± 0.04
Eticlopride	-7.64 ± 0.38	-7.98 ± 0.10

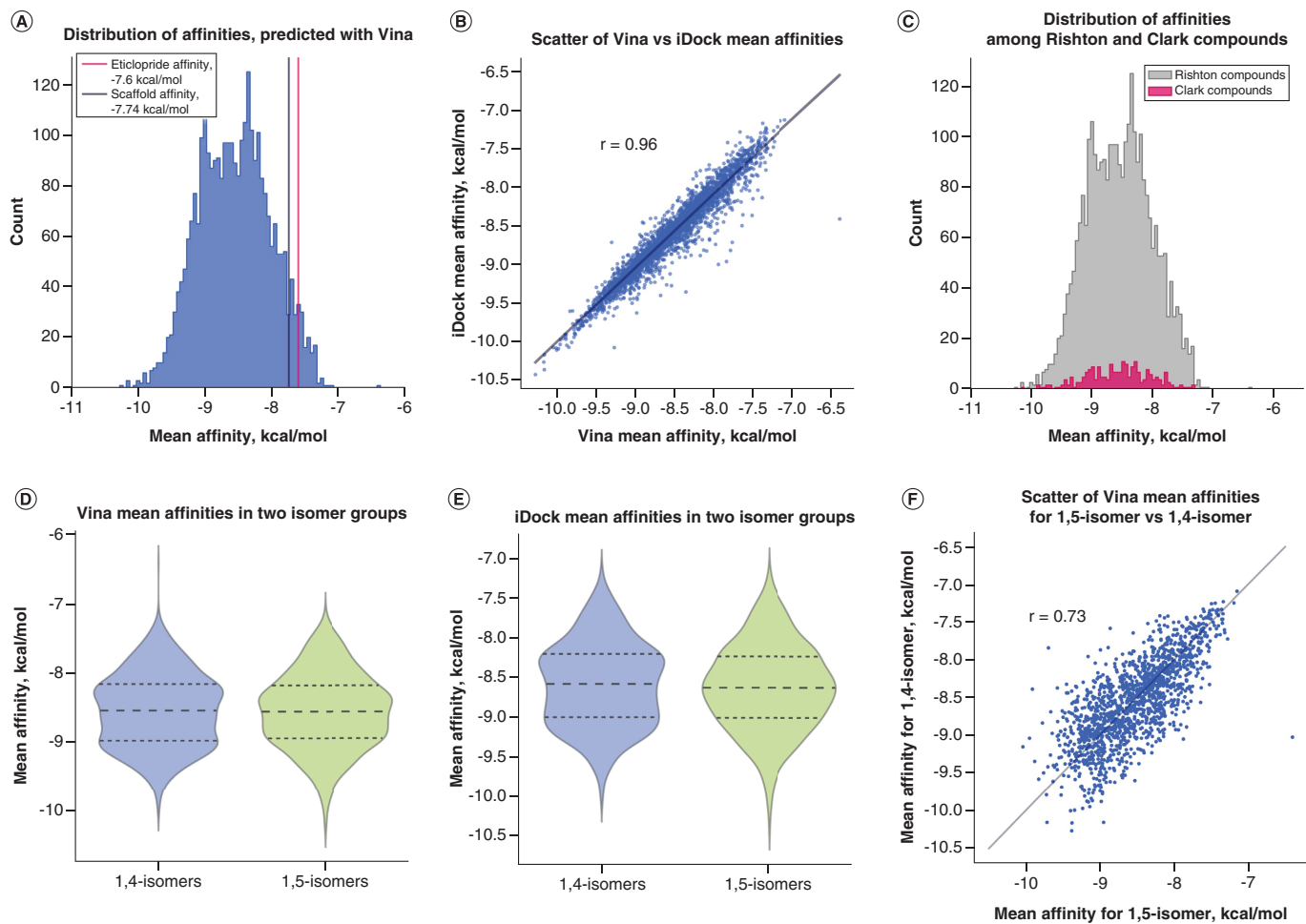


Figure 3. Vina and iDock binding affinities for 1,4- and 1,5-isomers. (A) The distribution of binding affinities predicted by Vina is shown, with threshold lines indicating the affinities of eticlopride (red line) and the scaffold (black line). (B) A scatter plot is presented, comparing the Vina mean affinities with the iDock affinities for the same molecules. The plot demonstrates a strong correlation between the two methods, with a Pearson's correlation coefficient of 0.96. (C) The distribution of predicted affinities using Vina is shown, with molecules grouped by their passing status in the Clark (red) and Rishton (gray) logarithmic ratio between the concentration of a compound in the brain and blood filtering. (D & E) Violin plots depicting the Vina and iDock affinities are presented, with a distinction made between 1,4-isomers (blue) and 1,5-isomers (green) using hue. The dashed lines highlight the quartiles of the distribution. (F) Scatter plot of Vina affinities in kcal/mol for 1,5-isomer molecules against values for 1,4-isomers of the same molecules (Pearson's $r = 0.73$).

dispersion of data points, indicating variations in binding affinities between different isomers (Figure 3F). However, there was no evidence to suggest any significant difference in binding affinity between the 1,4-isomers and the 1,5-isomers. Additionally, no correlations were observed between the ligands' binding affinities to the protein receptor and their Tanimoto similarities to the scaffold molecule and eticlopride (Supplementary Figures 2D & 3).

The top 10 molecules were identified with the lowest Vina and iDock affinities, all of which have positive logBB values ($\log\text{BB} > 0$). Notably, the majority of these molecules are 1,5-isomers (Table 2).

The binding modes observed for the 1,5-isomers listed in Table 2 predominantly exhibit similar conformations, with the 1,2,3-triazole ring oriented towards the binding pocket of eticlopride (Figure 4A). However, molecule 7000 deviates from this trend due to the presence of a large decahydronaphthalen-1-yl moiety, which forces this compound substructure to better occupy the binding site. In contrast, the ligand binding poses for the 1,4-isomers demonstrate different conformations within the binding pocket (Figure 4B), indicating that these molecules exhibit more flexibility in the binding site. Additionally, the incorporation of a radical group within the 1,2,3-triazole moiety allows for increased flexibility, enabling alterations in the molecular orientation. Finally, compound 7000 as a novel hit was selected for MD simulation due to its binding site occupancy within D3R, along with its low docking scores and high logBB values (Figure 4C).

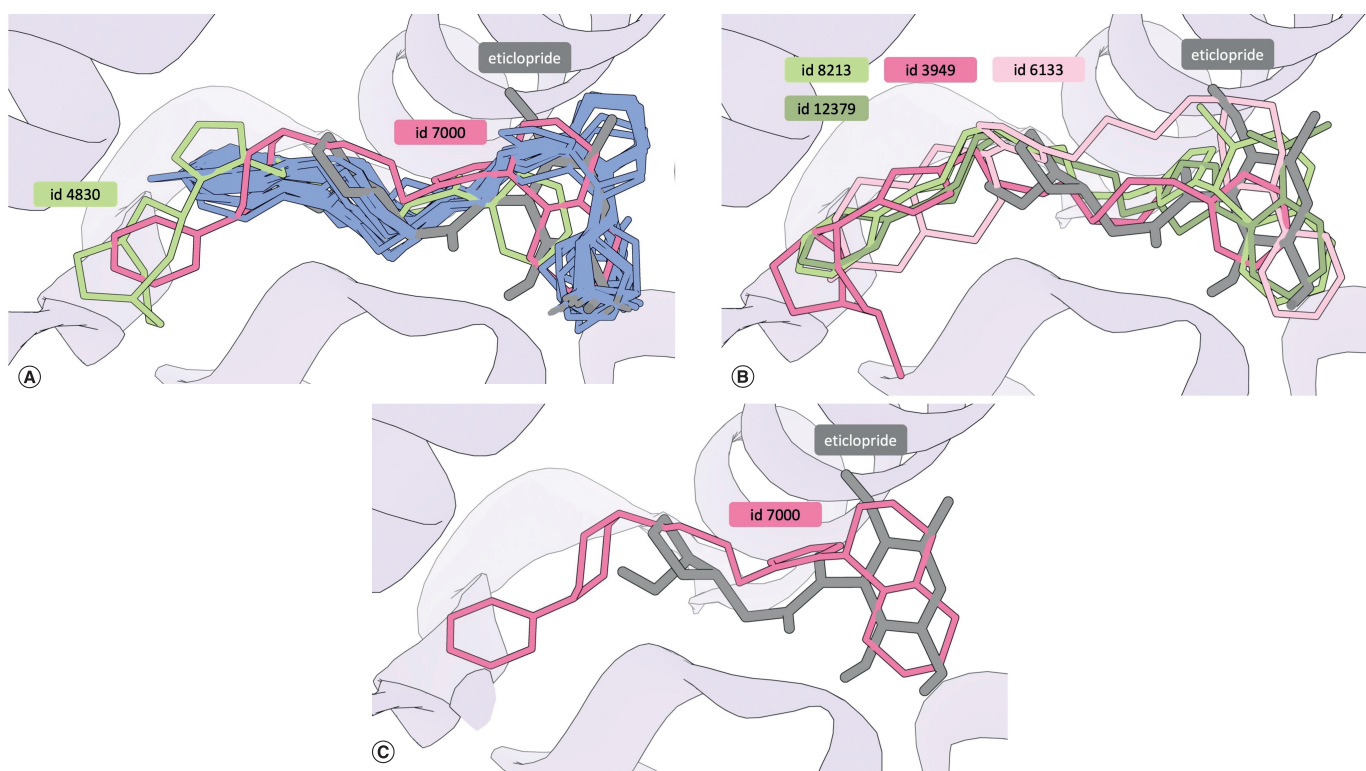


Figure 4. Binding modes for selected hits predicted by Vina. D3R helices are depicted in lavender; eticlopride is shown in gray. **(A)** Overlay of best binding modes for 1,5-isomers. The majority of molecules (blue) orient various radicals toward the binding pocket, whereas compounds 7000 (pink) and 4830 (green) have different conformations and occupy binding site. **(B)** Overlay of best binding modes for 1,4-isomers. Molecules 8213 (light green) and 12,379 (dark green) orient various radicals toward the binding pocket and molecules 3949 (pink) and 6133 (light pink) have inverted orientations. **(C)** Overlay of best binding modes for eticlopride and the compound (ID 7000) selected for molecular dynamics (pink).

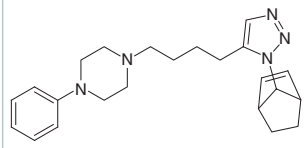
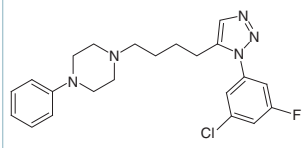
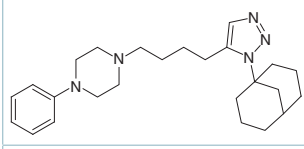
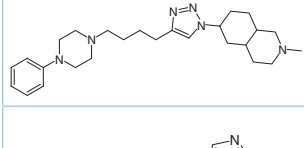
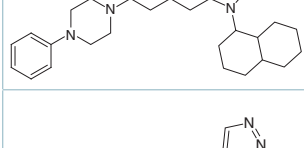
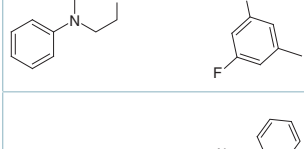
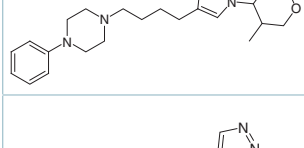
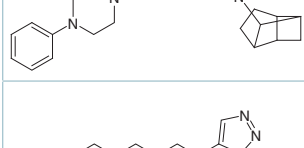
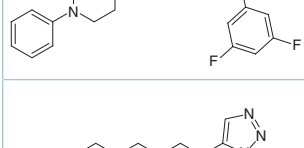
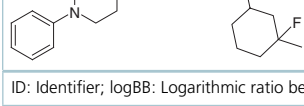
ID: Identifier.

To validate the previous observations and assess the protein-ligand interaction in a realistic environment, the binding affinities of the hit molecule and eticlopride to the human D3R protein were determined using a 200-ns MD simulation conducted with the AMBER software. The simulations considered the protein-ligand complexes embedded in a lipid membrane, mimicking the aqueous environment (Figure 5A & B). The analysis was performed by obtaining van der Waals and electrostatic interaction energies, where the average ΔG_{lie} values were found to be -60.17 kcal/mol for the novel hit and only -58.37 kcal/mol for the reference (Figure 6A). In addition, the ΔE_{vdW} component was detected below the energy threshold (-50 kcal/mol) for only the novel hit, contributing mainly to protein–ligand affinity (Figure 6B & C). By contrast, the ΔE_{elec} component was determined to be within the energy threshold (-100 kcal/mol) and quite similar for both ligands, probably because of their cationic nature. Therefore, ΔG_{lie} estimation from MD simulation supports molecule 7000 as a hit capable of effective D3R binding.

Materials & methods

With regard to library preparation and logBB estimation, the molecular library for screening was generated using an in-house Python3 code in Jupyter Notebook and is provided in the Supplementary Figures. The RDKit Python library (v.2020.09.1.0) was utilized for molecule handling, descriptor calculation and generation of click reaction products. A total of 143,075 azide molecules as SMILES strings were compiled through an extensive PubChem search. SMILES strings were filtered to have less than 30 but more than ten symbols in order to limit the size of the molecules in the library. In addition, the following SMILES were dropped: strings containing more than one species (such strings have the symbol ".")¹, strings containing more than one or no azide moiety and strings with an azide group not matching $\text{N} = [\text{N}^+] = [\text{N}^-]$. The filtered azide reagents were combined with the alkyne scaffold by running a reaction in RDKit via the SMARTS pattern. Subsequently, the products were filtered to satisfy Lipinski's rule of no more than five hydrogen bond donors, no more than ten hydrogen bond acceptors, molecular mass <500

Table 2. Top 10 binding molecules according to their affinities to dopamine receptor 3.

Compound structure	ID	Mean affinity Vina, kcal/mol	Mean affinity iDock, kcal/mol	logBB Clark	logBB Rishton
	134	-10.01	-10.08	0.13	0.34
	2304	-9.95	-9.98	0.23	0.44
	3700	-9.98	-10.09	0.27	0.49
	6133	-10.04	-10.08	0.11	0.34
	7000	-10.16	-10.17	0.34	0.56
	7788	-10.17	-10.26	0.18	0.39
	8213	-9.96	-10.03	0.07	0.33
	10844	-10.27	-10.42	0.14	0.36
	15848	-10.0	-10.11	0.15	0.36
	17806	-10.16	-10.36	0.24	0.45

ID: Identifier; logBB: Logarithmic ratio between the concentration of a compound in the brain and blood.

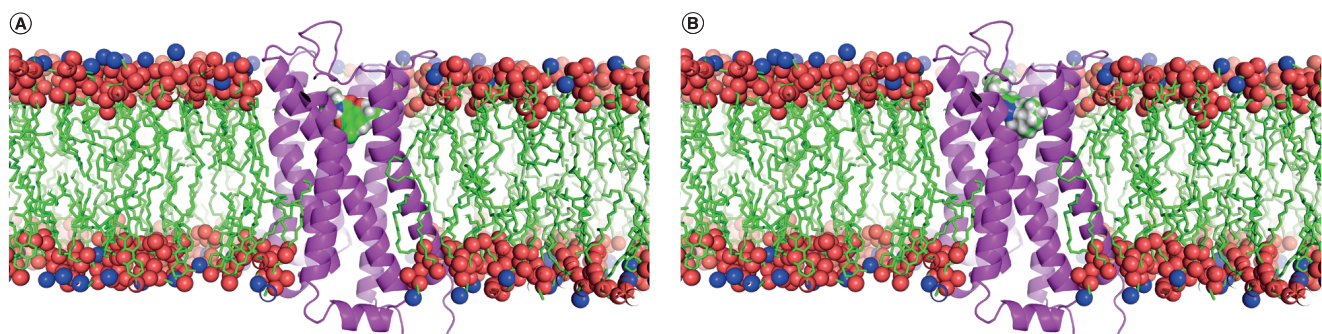


Figure 5. Protein–ligand–membrane systems analyzed in molecular dynamics simulations. Protein–ligand systems embedded in POPC:POPE:cholesterol (100:100:50) bilayer, including (A) eticlopride and (B) novel hit. All hydrogen molecules except the ligands are omitted to enhance clarity.

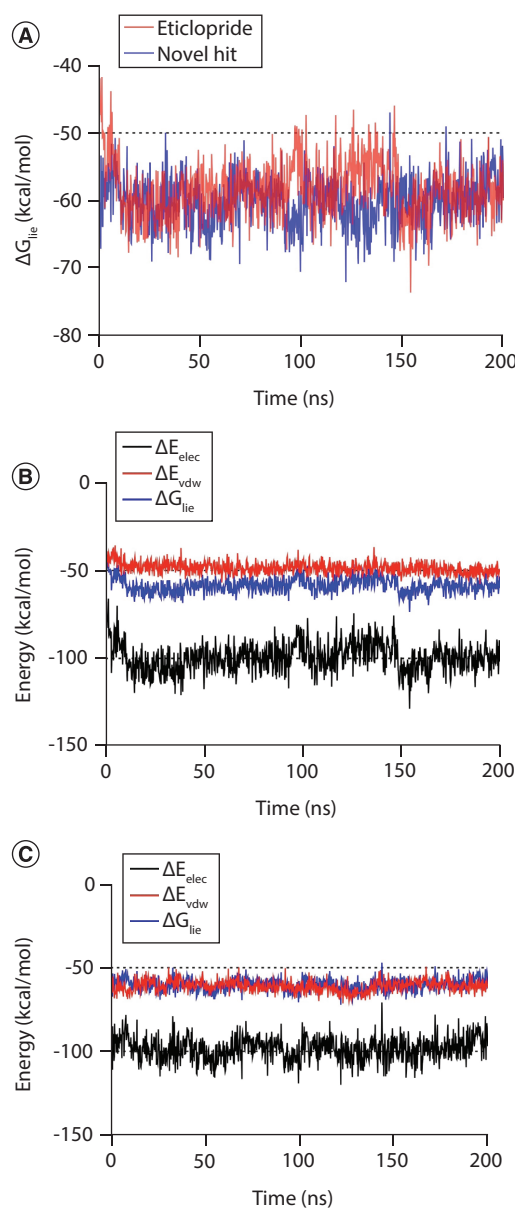


Figure 6. Binding energies for analyzed protein-ligand complexes in molecular dynamics simulations. (A) Linear interaction energy (ΔG_{liq}) plot based on van der Waals (ΔE_{vdW}) and electrostatic (ΔE_{elec}) interactions measured for the (B) reference molecule and (C) novel hit compound during the 200-ns molecular dynamics simulation as D3R antagonists. The energy thresholds are shown as dashed lines.

Da and partition coefficient ≤ 5 . The distribution of the number of rotatable bonds across generated compounds was calculated. In addition, for each product, the Tanimoto similarity was computed in relation to the scaffold and the reference D3R ligand, eticlopride. Next, logBB values were calculated for each compound with Clark and Rishton equations using the calculated octanol-water partition coefficient (ClogP) and topological polar surface area (TPSA), which were calculated in RDKit as descriptors:

$$\text{logBBClark} = 0.152 \cdot \text{ClogP} - 0.0148 \cdot \text{TPSA} + 0.139$$

$$\text{logBBRishton} = 0.155 \cdot \text{ClogP} - 0.01 \cdot \text{TPSA} + 0.164$$

Molecules readily permeable through the BBB were filtered by a logBB threshold of 0.3. Molecules passing the logBB filter as calculated by either the Clark or Rishton model were subjected to molecular docking screening.

The crystal structure of D3R complexed with eticlopride (PDB: 3PBL) served as the reference structure for conducting molecular docking experiments [27]. The protein was prepared for docking with AutoDockTools4 as a rigid receptor following the software manual [28]. For each molecule, three distinct conformations in MOL2 format were generated from the SMILES string by Open Babel v.3.1.0 [29] using MMFF94 force field geometry optimization invoked by the 'gen3d' key with the 'slow' option. Subsequently, Gasteiger charges were computed and each MOL2 conformation was converted to PDBQT format in Open Babel. Two software programs were utilized for molecular docking: AutoDock Vina v.1.1.2 [30,31] and iDock v.2.2.3 [32]. For both programs, a 20-Å box was specified with the center of binding site, where eticlopride is located in the Protein Data Bank crystal structure. The best binding modes were chosen according the docking affinities in kcal/mol. This analysis was also carried out for the scaffold molecule and eticlopride as reference molecules. Preparation of molecules and docking were performed on a Linux server with 20 central processing units per docking run. In-house Python3 scripts were used to run Open Babel, Vina and iDock algorithms. The scripts are provided in the Supplementary Figures. All docking scores were processed and plotted with an in-house Python3 code in Jupyter Notebook and are provided in the Supplementary Figures. A panel of hits was created by selecting the top 10 molecules with the lowest docking affinities predicted by the Vina and iDock algorithms. Finally, the best candidate (novel hit) for MD simulation was chosen.

The compound 1-{4-[1-(decahydronaphthalen-1-yl)-1H-1,2,3-triazol-5-yl]butyl}-4-phenylpiperazine was prepared for MD simulation (identifier 7000). Eticlopride was simulated as the reference ligand as well. The POPC:POPE:cholesterol (100:100:50) bilayer was built using the CHARMM-GUI pipeline, which was designed to generate membrane-bound protein structures. For orientation of the protein, 'align the first principal axis' was aligned along the Z-axis. The system was solvated according to the standard MD protocol published elsewhere [33]. All MD simulations were performed using the AMBER 20 package [34], with lipid14, ff99SB and GAFF force fields for the membrane, protein and ligand, respectively. The antechamber module of AmberTools was employed to calculate the AM1-BCC charges for the ligands. Cl anions were added to neutralize the solvated membrane–protein–ligand system (Figure 6A & B). Long-range electrostatic interactions were modeled via the particle mesh Ewald method. The SHAKE algorithm was applied to constrain the length of covalent bonds, including hydrogen atoms. The standard MD protocol included minimization (10,000 cycles), heating (5 ns), equilibration (5 ns) of periodic box dimensions and production (200 ns) with constant pressure. Finally, the linear interaction energy method was implemented to calculate binding free energy (ΔG_{lie}) using the equation

$$\Delta G_{\text{lie}} = \alpha \cdot E_{\text{vdW}} + \beta \cdot \Delta E_{\text{elec}}$$

where ΔE_{vdW} is the difference between van der Waals terms for protein-ligand and ligand–water interactions and ΔE_{elec} is the difference between electrostatic terms for protein-ligand and ligand–water interactions with default scaling factors ($\alpha = 0.18$; $\beta = 0.5$) [35].

Conclusion

This study presents an algorithm that utilizes a click reaction-based approach augmented by the BBB permeation analysis for the virtual screening of novel ligands targeting the D3R receptor. The algorithm involves the generation of drug-like molecules using in silico click reaction within the RDKit software. The workflow aims to select BBB-

permeable molecules by filtering according to logBB values computed by Clark and Rishton models. The analysis of D3R docking affinities for synthesized compounds suggests that filtering by Rishton's logBB is more beneficial, as it provides a larger set of BBB permeants for screening without compromising the proportion of affine binders. The comparison of docking scores between 1,4- and 1,5-isomers demonstrates that, despite possible differences in affinities for isomers of the same molecule, there is no general binding preference for a particular isomer, although the analysis of binding modes for top 10 1,5- and 1,4-isomer molecules highlights that 1,4-isomers are probably more flexible in the binding site. The 1,5-isomer hit (identifier 7000) was selected due to its high affinity and superior BBB permeability. To gain further insights, a 200-ns MD simulation of the membrane-embedded D3R complex was conducted to compare its behavior with that of eticlopride. The ΔG_{lie} estimation proved effective binding of the novel hit (-60.17 kcal/mol) in comparison with the reference (-58.37 kcal/mol), which is mainly due to lower ΔE_{vdW} of the 1,2,3-triazole molecule. Our next step involves experimental testing of the newly identified hit by measuring its binding affinity with the D3R receptor. Additionally, the established screening protocol can be utilized to effectively screen and evaluate new ligands that are synthesizable using combinatorial click chemistry. This approach holds promise for facilitating the discovery of potential D3R ligands with improved D3R binding and BBB permeation properties..

Executive summary

- Our novel algorithm combines click reaction and pharmacokinetic properties, specifically blood–brain barrier (BBB) permeation, for virtual screening of dopamine receptor 3 (D3R) ligands.
- BBB permeation criteria were based on the logarithmic ratio between the concentration of a compound in the brain and blood according to the Clark and Rishton models.
- A library of 1,2,3-triazole compounds was generated by combining an alkyne template with a collection of azides obtained from the PubChem database.
- The 1,5-isomer hit (identifier 7000) was chosen based on high affinity and best BBB permeability.
- Based on molecular dynamics simulation of the D3R membrane-embedded complex, free binding energy estimation with the linear interaction energy (ΔG_{lie}) method proved the hit's superior affinity over the reference ligand.
- A workflow for *in silico* screening of D3R ligands with BBB permeation aided by *in silico* click reaction is described and validated.

Supplementary data

To view the supplementary data that accompany this paper please visit the journal website at: www.future-science.com/doi/suppl/10.4155/fmc-2022-0310

Author contributions

S Shityakov conceived and supervised the project. AA Kovalenko prepared the library, performed docking screening and visualization and wrote the original draft. S Shityakov, YB Porozov and EV Skorb were responsible for the methodology, conducted molecular dynamics simulation and analysis and reviewed and edited the manuscript. All authors have approved the final version of the manuscript.

Financial & competing interests disclosure

The authors would like to express their sincere gratitude for the support received from the FSER-2021-0013 project, the ITMO Fellowship program, and the academic leadership program Priority 2030 proposed by the Federal State Autonomous Educational Institution of Higher Education IM Sechenov First Moscow State Medical University of the Ministry of Health of the Russian Federation. The assistance provided by these programs has been instrumental in establishing the necessary research infrastructure for conducting this study.

The authors have no other relevant affiliations or financial involvement with any organization or entity with a financial interest in or financial conflict with the subject matter or materials discussed in the manuscript apart from those disclosed.

No writing assistance was utilized in the production of this manuscript.

Availability of data & materials

The study employed various Python scripts for different purposes. These include a script with SMILES strings of azides for library construction, a Jupyter Notebook dedicated to library preparation and molecular property calculation, and a separate

script for handling the properties of 1,2,3-triazole compounds stored in a .csv format. Additionally, the repository on GitHub (<https://github.com/Aleksandr-biochem?tab=repositories>) provides access to supplementary Python scripts for setting up and executing docking jobs. These resources are freely available for researchers to utilize.

References

Papers of special note have been highlighted as: • of interest

- Leggio GM, Bucolo C, Platania CBM, Salomone S, Drago F. Current drug treatments targeting dopamine D3 receptor. *Pharmacol. Ther.* 165, 164–177 (2016).
- Beaulieu J-M, Gainetdinov RR. The physiology, signaling, and pharmacology of dopamine receptors. *Pharmacol. Rev.* 63(1), 182–217 (2011).
- Nicola SM, Surmeier DJ, Malenka RC. Dopaminergic modulation of neuronal excitability in the striatum and nucleus accumbens. *Annu. Rev. Neurosci.* 23(1), 185–215 (2000).
- Sokoloff P, Giros B, Martres MP, Bouthenet ML, Schwartz JC. Molecular cloning and characterization of a novel dopamine receptor (D3) as a target for neuroleptics. *Nature* 347(6289), 146–151 (1990).
- Heidbreder C. Selective antagonism at dopamine D3 receptors as a target for drug addiction pharmacotherapy: a review of preclinical evidence. *CNS Neurol. Disord. Drug Targets* 7(5), 410–421 (2008).
- Collo G, Zanetti S, Missale C, Spano P. Dopamine D3 receptor-preferring agonists increase dendrite arborization of mesencephalic dopaminergic neurons via extracellular signal-regulated kinase phosphorylation. *Eur. J. Neurosci.* 28(7), 1231–1240 (2008).
- Bellucci A, Collo G, Sarnico I, Battistin L, Missale C, Spano P. Alpha-synuclein aggregation and cell death triggered by energy deprivation and dopamine overload are counteracted by D2/D3 receptor activation. *J. Neurochem.* 106(2), 560–577 (2008).
- Kawano M, Sawada K, Tsuru E et al. Dopamine receptor D3R and D4R mRNA levels in peripheral lymphocytes in patients with schizophrenia correlate with severity of illness. *Open J. Psychiatry* 1(02), 33 (2011).
- Yang P, Perlmuter JS, Benzingier TL, Morris JC, Xu J. Dopamine D3 receptor: a neglected participant in Parkinson disease pathogenesis and treatment? *Ageing Res. Rev.* 57, 100994 (2020).
- Heidbreder CA, Newman AH. Current perspectives on selective dopamine D3 receptor antagonists as pharmacotherapeutics for addictions and related disorders. *Ann. N. Y. Acad. Sci.* 1187(1), 4–34 (2010).
- Moraga-Amaro R, Gonzalez H, Pacheco R, Stehberg J. Dopamine receptor D3 deficiency results in chronic depression and anxiety. *Behav. Brain Res.* 274, 186–193 (2014).
- Bucolo C, Leggio GM, Drago F, Salomone S. Dopamine outside the brain: the eye, cardiovascular system and endocrine pancreas. *Pharmacol. Ther.* 203, 107392 (2019).
- Sokoloff P, Diaz J, Foll BL et al. The dopamine D3 receptor: a therapeutic target for the treatment of neuropsychiatric disorders. *CNS Neurol. Disord. Drug Targets* 5(1), 25–43 (2006).
- Newman AH, Grundt P, Cyriac G et al. *N*-(4-(4-(2,3-dichloro- or 2-methoxyphenyl)piperazin-1-yl)butyl)heterobiarylcarboxamides with functionalized linking chains as high affinity and enantioselective D3 receptor antagonists. *J. Med. Chem.* 52(8), 2559–2570 (2009).
- Banala AK, Levy BA, Khatri SS et al. *N*-(3-fluoro-4-(4-(2-methoxy or 2,3-dichlorophenyl)piperazine-1-yl)butyl)arylcarboxamides as selective dopamine D3 receptor ligands: critical role of the carboxamide linker for D3 receptor selectivity. *J. Med. Chem.* 54(10), 3581–3594 (2011).
- Michino M, Donthamsetti P, Beuming T et al. A single glycine in extracellular loop 1 is the critical determinant for pharmacological specificity of dopamine D2 and D3 receptors. *Mol. Pharmacol.* 84(6), 854–864 (2013).
- Keck TM, Banala AK, Slack RD et al. Using click chemistry toward novel 1,2,3-triazole-linked dopamine D3 receptor ligands. *Bioorg. Med. Chem.* 23(14), 4000–4012 (2015).
- Vass M, Schmidt É, Horti F, Keserű GM. Virtual fragment screening on GPCRs: a case study on dopamine D3 and histamine H4 receptors. *Eur. J. Med. Chem.* 77, 38–46 (2014).
- Lee JH, Cho SJ, Kim M-H. Discovery of CNS-like D3R-selective antagonists using 3D pharmacophore guided virtual screening. *Molecules* 23(10), 2452 (2018).
- Byvatov E, Sasse BC, Stark H, Schneider G. From virtual to real screening for D3 dopamine receptor ligands. *Chembiochem* 6(6), 997–999 (2005).
- Shityakov S, Förster C. *In silico* predictive model to determine vector-mediated transport properties for the blood–brain barrier choline transporter. *Adv. Appl. Bioinform. Chem.* 7, 23–36 (2014).
- Shityakov S, Salmas RE, Durdagı S et al. Characterization, *in vivo* evaluation, and molecular modeling of different propofol–cyclodextrin complexes to assess their drug delivery potential at the blood–brain barrier level. *J. Chem. Inf. Model.* 56(10), 1914–1922 (2016).
- Molecules with high permeability through the blood-brain barrier (BBB) were selected using a logBB threshold of 0.3, a criterion that has been supported and validated by Shityakov et al. in 2016.**

23. Clark DE. Rapid calculation of polar molecular surface area and its application to the prediction of transport phenomena. 2. Prediction of blood-brain barrier penetration. *J. Pharm. Sci.* 88(8), 815–821 (1999).
24. Rishton GM, Labonte K, Williams AJ, Kassam K, Kolovanov E. Computational approaches to the prediction of blood-brain barrier permeability: a comparative analysis of central nervous system drugs versus secretase inhibitors for Alzheimer's disease. *Curr. Opin. Drug Discov. Devel.* 9(3), 303–313 (2006).
25. Günther S, Senger C, Michalsky E, Goede A, Preissner R. Representation of target-bound drugs by computed conformers: implications for conformational libraries. *BMC Bioinformatics* 7(1), 1–11 (2006).
26. Kunwittaya S, Nantasesamat C, Treeratanapiboon L, Srisarin A, Isarankura-Na-Ayudhya C, Prachayasittikul V. Influence of logBB cut-off on the prediction of blood-brain barrier permeability. *Biomed. Appl. Technol. J.* 1, 16–34 (2013).
27. Chien EY, Liu W, Zhao Q *et al.* Structure of the human dopamine D3 receptor in complex with a D2/D3 selective antagonist. *Science* 330(6007), 1091–1095 (2010).
28. Morris GM, Huey R, Lindstrom W *et al.* AutoDock4 and AutoDockTools4: automated docking with selective receptor flexibility. *J. Comput. Chem.* 30(16), 2785–2791 (2009).
29. O'Boyle NM, Banck M, James CA, Morley C, Vandermeersch T, Hutchison GR. Open Babel: an open chemical toolbox. *J. Cheminform.* 3(1), 1–14 (2011).
30. Trott O, Olson AJ. AutoDock Vina: improving the speed and accuracy of docking with a new scoring function, efficient optimization, and multithreading. *J. Comput. Chem.* 31(2), 455–461 (2010).
31. Eberhardt J, Santos-Martins D, Tillack AF, Forli S. AutoDock Vina 1.2.0: new docking methods, expanded force field, and Python bindings. *J. Chem. Inf. Model.* 61(8), 3891–3898 (2021).
32. Li H, Leung K-S, Wong M-H. iDock: a multithreaded virtual screening tool for flexible ligand docking. In: *2012 IEEE Symposium on Computational Intelligence in Bioinformatics and Computational Biology*. Institute of Electrical and Electronics Engineers, CA, USA, 77–84 (2012).
33. Kučerka N, Tristram-Nagle S, Nagle JF. Structure of fully hydrated fluid phase lipid bilayers with monounsaturated chains. *J. Membr. Biol.* 208, 193–202 (2006).
34. Case D, Belfon K, Ben-Shalom I *et al.* AMBER 2020. University of California, CA, USA (2020).
35. Shityakov S, Roewer N, Förster C, Broscheit J-A. *In silico* investigation of propofol binding sites in human serum albumin using explicit and implicit solvation models. *Comput. Biol. Chem.* 70, 191–197 (2017).
36. Tomasello G, Armenia I, Molla G. The Protein Imager: a full-featured online molecular viewer interface with server-side HQ-rendering capabilities. *Bioinformatics* 36(9), 2909–2911 (2020).